



**RESEARCH ARTICLE**

**CHEMICAL AND MINERALOGICAL ANALYSES OF THE LATE NEOLITHIC  
CERAMICS FROM ŞAH VALLEY (SINGUBER), TURKEY**

Murat BAYAZIT<sup>1\*</sup>, Esra KAYNAK<sup>2</sup>, Nilgün COŞKUN<sup>3</sup>

<sup>1\*</sup>Batman University, Faculty of Fine Arts, Department of Ceramics, Batı Raman Campus, Batman, [m.bayazit@hotmail.com](mailto:m.bayazit@hotmail.com),  
ORCID: 0000-0003-1453-249X

<sup>2</sup>Batman University, Received M.Sc. at Department of Archaeometry, Institute of Science, [esrakaynakk@hotmail.com](mailto:esrakaynakk@hotmail.com),  
ORCID: 0000-0002-1070-957X

<sup>3</sup>Hatay Mustafa Kemal University, Faculty of Letters, Department of Archaeology, Hatay, [nilguncoskun@yahoo.com](mailto:nilguncoskun@yahoo.com), ORCID:  
0000-0003-0848-9413

*Receive Date: 18.11.2022*

*Accepted Date: 23.03.2023*

**ABSTRACT**

Numerous settlements have been identified during the surveys in Şırnak province (Turkey) since the beginning of the 19th century. The potsherds found in the central of such settlements have been thought to be affected by Mesopotamian culture, and the ones from the hillside of the Şah Valley were considered as the most eastern examples of the Hassuna Samara culture. This study presents the results regarding one of the first detailed archaeometric investigations carried out for the Late Neolithic ceramic findings unearthed from Şah Valley (Şırnak province, Turkey). The ceramics were initially characterized by means of portable X-ray fluorescence (p-XRF) and X-ray diffraction (XRD) in order to enlighten the chemical and mineralogical features of the samples, respectively. The results indicated use of calcareous raw material sources and a low firing temperature range (ca. 700-800°C). The potsherds were also investigated through petrography which showed the presence of quartz, opaque minerals, plagioclase and biotite as the minerals, and clay, claystone and marl rock contents as the rock types for the samples, in general. Fourier transformed infrared (FTIR) spectroscopy was additionally applied for the potsherds. This complementary technique provided information about the vibrations of the chemical bands in the ceramics which displayed the characteristic bond vibrations of decisive minerals in the ceramic fabrics, such as calcite, clay minerals and quartz. Considering the whole archaeometric data, it can be deduced that the Neolithic ceramics of the Şah Valley have been subjected to low firing temperatures which could be assigned to a basic production procedure presumably claiming daily-use wares.

**Keywords:** *Materials characterization, Archaeometry, Late Neolithic, Ceramics, Şah Valley.*

**1. INTRODUCTION**

When the archaeological excavations are examined in general, the most numerous finds among the materials unearthed are the ceramics. The word "ceramic" is derived from the Greek word "Keramos"

meaning "burnt material" and is defined as the material obtained as a result of shaping the compositions of inorganic materials after they gain a certain plasticity, drying and firing them until they reach sufficient hardness and strength. The main raw materials of the ceramic are clay, quartz and feldspars. In general, ceramic materials obtained as a result of shaping the soil with water and baking it with fire to obtain the ultimate product have been used by people for many different purposes throughout the history. Thus, ancient ceramic materials are of great importance in terms of history of humanity, and therefore archaeology. Especially in the last century archaeometric studies, which include engineering and science (as well as archaeology, art history), have recently become widespread and are used to reveal the characteristic features of ancient artifacts (e.g. ceramics, metal, glass, tile etc.) [1-4].

Ceramics, which started with the terracotta products of the Neolithic Period between 8000-5500 BC and showed a continuous development in parallel with the way of life of human beings from the beginning of the ceramic period in Anatolia, have constantly renewed and developed themselves. With the industrial revolution, ceramic materials showed themselves in various fields such as automotive, space crafts, sanitary wares, wearable technologies, which require an advanced technology. According to today's archaeological data, the Neolithic Period, dated approximately between 10000 BC and 6000 BC, is one of the most important eras in human history, since the Neolithic Period is an indication of the transition to settled life and the foundation of today's life [5-7].

The southeastern Anatolia region is geographically located between the southern part of the southeast Taurus Mountains in Anatolia and the border of Syria and Iraq. Southeastern Anatolia region is the widest part of the area called "Fertile Crescent" (Mediterranean in the west, Zagros Mountains in the east, Southeast Taurus Mountains in the north and Arabian Desert in the south). This strategic area, where different civilizations intersect, was frequently used by caravans trading between Mesopotamia, Syria and Anatolia, by nomads doing animal husbandry and also by societies organizing expeditions. Şırnak, located at the northeastern end of the Fertile Crescent, is surrounded by Namaz Mountain, which is connected to the southeast Taurus Mountains (from the north), Gabar Mountain (from the west), and Cudi Mountain (from the southeast). Şırnak and its surroundings appear as a crossroads in the Neolithic Period [8-11].

The earliest painted pottery cultures of Northern Mesopotamia are traced in the period called Hassuna Samarra or Late Neolithic-4, which dates back to about 8000 years ago. These painted potteries were named after the centers where they were found for the first time. The pottery, all of which are hand-formed, may be light brown, cream, beige paste, mostly unslipped, and contain sand, plant and sometimes grit tempered. Their surfaces are generally lightly burnished and smoothed. This type of pottery was found in Salat Mosque and Hakemi Use, among the excavations carried out in the Upper Tigris Valley, in the easternmost part of the Southeast Anatolian Region [12,13].

Within the scope of this study, a research was conducted including the archaeometric characterization of 30 ceramic samples dated to the Neolithic Period, which are the easternmost examples of Hassuna Samarra culture in the slope settlement of Şah Valley (Şırnak) (Figure 1) [8], and thus, it is aimed to contribute to the existing literature. The ceramic group, which is the subject of this study, was found in the settlement determined during the Şırnak Province Center, Güçlükönak, Uludere and

Beytüşşebap Districts Survey conducted by the team headed by Nilgün Coşkun (Hatay Mustafa Kemal University) with the permission of Ministry of Culture and Tourism, Turkey. The ceramic findings were analyzed by means of portable X-ray fluorescence (p-XRF), X-ray diffraction (XRD), optical microscope (petrography) and Fourier transformed infrared (FTIR) spectroscopy, which are frequently employed for ceramic findings.

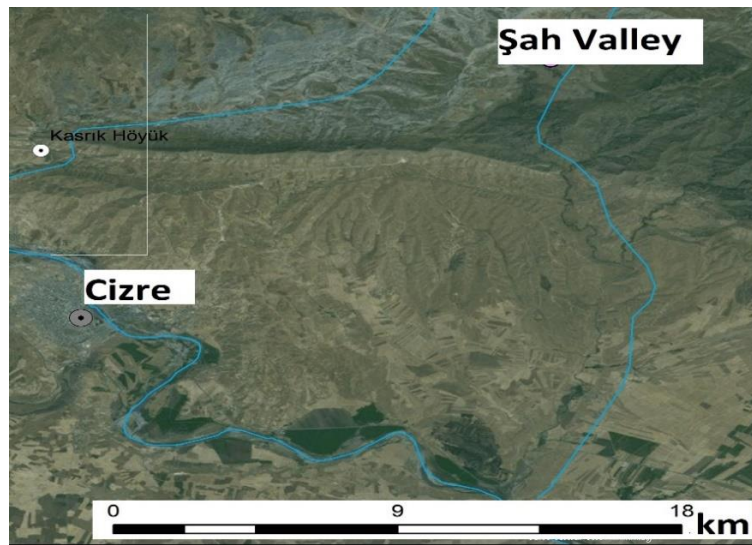
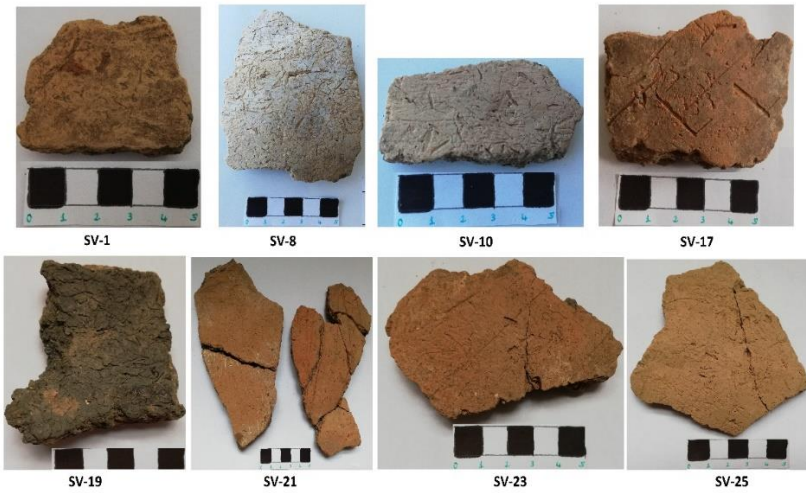


**Figure 1.** Location of Şah Valley [8].

## 2. EXPERIMENTAL

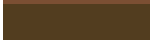
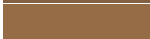
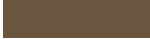
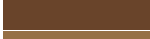
### 2.1. Sampling

30 potsherds representing the Neolithic ceramics of Şah Valley were selected among the amorphous potsherds (considering form, color, etc.) by Assoc. Prof. Dr. Nilgün (Masatcıoğlu) Coşkun, the scientific advisor of "Sırnak Province Center, Güçlükonak, Uludere and Beytüşşebap Districts Survey" (Şırnak İli Merkez, Güçlükonak, Uludere ve Beytüşşebap İlçeleri Yüzey Araştırması, in Turkish). Some of the representative samples are given in Figure 2 (sample code abbreviation is SV, Şah Valley).



**Figure 2.** Some of the representative Neolithic ceramics analyzed in the study.

**Table 1.** L, a, b values and Equivalent colors of the potsherds.

Sample	L	a	b	Equivalent color
SV-1	40.82	4.26	17.40	
SV-2	48.39	7.79	27.81	
SV-3	37.91	15.33	24.01	
SV-4	27.38	5.17	21.83	
SV-5	40.22	6.79	19.65	
SV-6	46.38	12.79	25.87	
SV-7	33.59	14.94	28.34	
SV-8	29.24	10.89	18.32	
SV-9	43.49	9.74	23.03	
SV-10	49.08	12.20	27.19	
SV-11	42.07	10.77	21.13	
SV-12	36.54	12.13	20.23	
SV-13	43.32	5.87	20.31	
SV-14	44.85	8.59	23.08	
SV-15	42.39	10.20	23.90	
SV-16	37.78	5.60	16.86	
SV-17	37.42	7.25	21.26	
SV-18	38.27	10.58	21.93	
SV-19	20.05	10.36	20.70	
SV-20	38.87	6.42	19.60	
SV-21	31.38	7.28	19.22	
SV-22	42.45	-1.55	18.90	
SV-23	42.66	8.20	21.27	
SV-24	45.89	15.41	28.20	
SV-25	35.42	6.11	20.34	
SV-26	28.35	12.37	19.68	
SV-27	44.74	15.73	27.25	
SV-28	45.28	11.62	27.82	
SV-29	32.49	12.91	22.12	
SV-30	50.09	9.71	29.58	
<i>Mean</i>	<i>39.23</i>	<i>9.52</i>	<i>22.56</i>	

L: White/black (0/100), a: green (0/-60) and red (0/+60), b: blue (b: 0/-60) and yellow (0/+60).

Ceramic samples were kept in distilled water for 24-48 hours considering the contamination status. These impurities were softened and separated from the sample surface. Visible impurities were removed from the surface with the help of a scalpel and the samples were ground into powder in a porcelain mortar in order to use in XRD and FTIR. Bulk samples were used in p-XRF and petrography. After the cleaning process, the equivalent colors of the ceramics were determined. For this purpose, CIA L, a, b values (Commission Internationale de L'Eclairage color system) in ceramics were determined with the ColorQA Pro System III program with a portable colorimeter (Table 1).

## **2.2. Analyses**

In the present study, the chemical compositions of 30 samples were examined with the INNOVX model OLYMPUSX portable XRF device. Analyzes were performed in GeoChem mode. The elements that can be scanned in the first scattering (40 kV) in the analyzes made in the Geochem mode of the device are Zn, Pt, W, Au, Br, Pb, Bi, Rb, Hg, As, V, Cr, Fe, Mn Co, Ni, Cd, Sn, Sb, Ti Cu, Se, U, Sr, Y, Zr, Th, Nb, Mo, Ag. Elements within the scanning limit in the second scattering (10 kV) are Ca, Si, Mg, Al, P, Mn, K, S, Ti. Portable XRF was used as a non-destructive technique.

XRD analysis was used to detect the minerals in the ceramics and was performed with a Rigaku/Miniflex-2 XRD device. The goniometric speed was 2°/min and the scanning range was 5-50 2-theta, which is the range in which soil minerals can be detected. The anode in the device was CuK $\alpha$  (1.541871 Å) and analyzes were carried out under 35 kV voltage and 15 mA current. Powder samples were used in XRD analysis and no acidification was applied.

FTIR was employed as a complementary technique in the research. The analyses were carried out on the sample powders using a Perkin Elmer FTIR device. The spectra were taken between the wavenumbers of 650-4000 cm<sup>-1</sup>. The assignment of the bands for the minerals are made in the range of 650-1800 cm<sup>-1</sup> (the fingerprint region for the ceramics). The results were interpreted comparatively with the band values in the available literature. The petrographic analyzes of ceramics were performed with a DMLP model Leica Research Polarizing optical microscope. A Leica DFC280 digital camera was used to capture the images during the analyses. The camera has x25 magnification and works with both single and double nicol. A Leica Qwin digital imaging system was used to evaluate the images obtained for the ceramics. Point Counting method was applied in the determination of mineral/rock contents in the samples.

## **3. RESULTS AND DISCUSSION**

### **3.1. Portable XRF results**

The oxides detected in p-XRF analysis for the ceramics are given in Table 2, and variation of the oxides are given in Figure 3.

The high amount of CaO (27.83 wt. % on average) determined for the ceramics indicated that carbonates (i.e. calcite) were included in the raw materials used in production. The high values of CaO ratio also suggested that the amount of clay minerals in the raw material(s) was low. The amount of Al<sub>2</sub>O<sub>3</sub> determined in the ceramics (8.22 wt. % on average) supports this interpretation. It was seen that

the amount of SiO<sub>2</sub> in the ceramics was also relatively low (41.29 wt. % on average). These results indicated that the starting raw material of the ceramics would have a calcareous character. Taking into account the moderate and/or relatively high amounts of K<sub>2</sub>O, it can be deduced that potassium would have originated from the clay and/or feldspathic materials (K-feldspar or plagioclases). The low Al<sub>2</sub>O<sub>3</sub> content in the samples, on the other hand, indicated that the potassium oxide might have come mostly from feldspar or plagioclase. The ceramics with high MgO content were thought to possess dolomite which was presumably present as a carbonate raw material in addition to calcite [14,15].

**Table 2.** The oxides detected in ceramics by p-XRF.

Code	CaO	SiO <sub>2</sub>	Fe <sub>2</sub> O <sub>3</sub>	MgO	Al <sub>2</sub> O <sub>3</sub>	K <sub>2</sub> O <sub>5</sub>	P <sub>2</sub> O <sub>5</sub>	TiO <sub>2</sub>	MnO	Cr <sub>2</sub> O <sub>3</sub>
<b>SV- 1</b>	30.92	41.05	11.88	-	8.70	4.63	2.08	0.94	0.14	-
<b>SV- 2</b>	28.95	40.56	13.52	5.08	7.61	2.29	1.34	0.74	0.08	0.14
<b>SV- 3</b>	40.39	29.85	9.90	8.76	6.03	2.28	1.87	0.63	0.09	-
<b>SV- 4</b>	35.20	37.51	10.98	3.88	7.17	3.15	1.64	0.74	0.17	-
<b>SV- 5</b>	17.50	48.79	13.95	-	10.97	4.93	2.48	1.18	0.20	-
<b>SV- 6</b>	17.57	49.58	14.10	-	10.94	4.97	1.97	1.07	0.20	-
<b>SV- 7</b>	30.30	38.76	11.84	8	7.18	1.91	1.37	0.63	0.08	-
<b>SV- 8</b>	30.35	40.74	12.73	3.50	7.14	3.18	1.98	0.8	0.15	-
<b>SV- 9</b>	43.14	33.04	8.92	3.64	7.32	2.23	1.22	0.64	0.06	-
<b>SV- 10</b>	31.69	39.16	10.84	-	8.23	4.25	2.04	0.81	0.15	-
<b>SV- 11</b>	33.47	37.72	10.66	3.41	7.90	3.88	2.18	0.77	0.15	-
<b>SV- 12</b>	43.02	32.22	9.26	3.80	7.51	2.29	1.41	0.67	0.08	-
<b>SV- 13</b>	30.95	37.96	12.34	7.93	6.74	1.72	1.34	0.65	0.08	-
<b>SV- 14</b>	25.64	40.30	12.28	8.69	7.84	2.21	1.67	0.77	0.21	0.15
<b>SV- 15</b>	31.94	38.07	11.91	7.38	6.75	1.82	1.25	0.66	0.09	-
<b>SV- 16</b>	19.01	47.52	14.50	-	10.25	4.82	1.91	1.20	0.22	-
<b>SV- 17</b>	14.60	48.14	15.38	7.91	8.17	3.35	1.74	0.82	0.14	-
<b>SV- 18</b>	14.92	48.91	15.50	3.38	9.67	4.54	2.33	1.22	0.22	-
<b>SV- 19</b>	13.80	52.08	15.45	-	11.42	4.33	2.36	1.19	0.09	-
<b>SV- 20</b>	28.16	40.39	12.36	5.68	7.01	2.87	1.83	0.76	0.15	0.15
<b>SV- 21</b>	15.35	47.39	15.32	7.46	8.39	3.12	1.87	0.85	0.18	-
<b>SV- 22</b>	38.73	33.90	11.68	3.76	6.28	3.54	1.43	0.67	0.08	-
<b>SV- 23</b>	21.25	45.42	12.73	3.76	9.97	4.28	1.85	0.95	0.26	-
<b>SV- 24</b>	30.63	39.96	12.15	-	8.54	5.15	2.24	0.90	0.09	-
<b>SV- 25</b>	32.70	38.81	11.02	3.15	7.95	3.74	1.98	0.88	0.16	-
<b>SV- 26</b>	34.40	37.28	11.01	3.40	7.80	3.74	1.84	0.84	0.16	-
<b>SV- 27</b>	16.41	45.90	14.01	9.60	8.29	2.62	1.71	0.78	0.17	-
<b>SV- 28</b>	39.14	37.05	10.70	-	7.37	3.38	1.74	0.80	0.14	-
<b>SV- 29</b>	15.56	50.51	14.23	-	10.81	5.08	2.11	1.13	0.09	-
<b>SV- 30</b>	29.26	40.41	13.33	5.17	6.89	2.94	1.50	0.73	0.09	-
<b>Mean</b>	<b>27.83</b>	<b>41.29</b>	<b>12.48</b>	<b>5.58</b>	<b>8.22</b>	<b>3.44</b>	<b>1.80</b>	<b>0.84</b>	<b>0.13</b>	<b>0.14</b>

(-): not determined or below the detection limit (not included in the mean value).

It was predicted that the element that have provided the red and brown hues to the body was mainly iron, since no other colorant elements were not determined in the portable XRF analysis. As is known, iron oxides can give various colors in different firing atmospheres. Iron is oxidized in oxidizing firing atmosphere and turns into hematite resulting in reddish tones, whereas it is reduced in reducing firing atmosphere and turns into magnetite resulting in black tones [16].

The ceramics with black-gray tones of paste between two red-brown surfaces, or with layers that can be clearly distinguished as red and black inside and outside are referred as "sandwich structure" in the literature. The emergence of this type of structure mainly depends on the raw material and the firing conditions, and could be also due to addition of organic materials. In the present study, elongated and irregular voids were clearly observed on most of the ceramic surfaces, which were predicted to be formed as a result of removal of organic materials (e.g. straw, grass). Such additives could have been used as temper materials in order to strengthen the ceramic body. It could be deduced that organic additives would have been used in addition to iron content for the potsherds having sandwich structure in the present study [17].

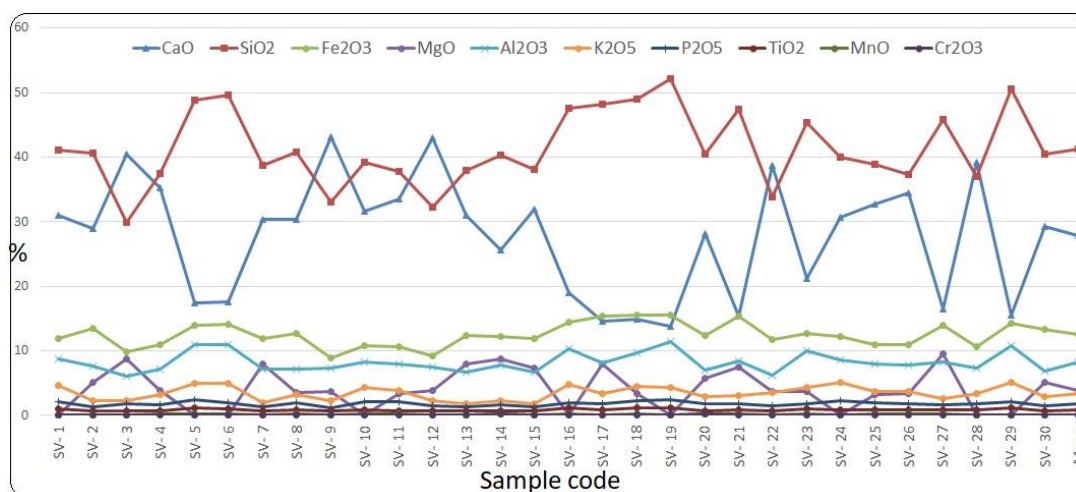


**Figure 3.** The variation of oxides in the samples.

The ceramics were classified through the hierarchical clustering analysis using SPSS 17.0. statistical program. The clustering analysis was initially applied considering the amounts of CaO, SiO<sub>2</sub>, Al<sub>2</sub>O<sub>3</sub>, Fe<sub>2</sub>O<sub>3</sub>, K<sub>2</sub>O and TiO<sub>2</sub> (Figure 4a). Then, only CaO, SiO<sub>2</sub> and Al<sub>2</sub>O<sub>3</sub> (having relatively higher ratios in p-XRF) were taken into account for the same analysis (Figure 4b). Absence of any significant difference between two dendrogram indicated that the starting raw materials used in the production of the ceramics mainly contain calcium, silica and alumina. It was observed that the ceramics were divided into two main groups in the clustering analysis performed through the oxide contents. The groups are as the followings;

**Group-1:** SV-5, SV-6, SV-16, SV-17, SV-18, SV-19, SV-21, SV-23, SV-27, SV-29 (CaO: 13.80-21.25 wt. %).

**Group-2:** SV-1, SV-2, SV-3, SV-4, SV-7, SV-8, SV-9, SV-10, SV-11, SV-12, SV-13, SV-14, SV-15, SV-20, SV-22, SV-24, SV-25, SV-26, SV-28, SV-30 (CaO: 25.64-43.14 wt. %).

As can be seen, the CaO content was decisive in the separation of ceramics into groups. Ceramics with the content of CaO between 13.80% and 21.25% formed the first group, and the ceramics with the content of CaO between 25.64% and 43.14% formed the second group. In any case, since the use of calcareous raw materials comes to the fore, it was foreseen that a similar or the same source, but varying in carbonate raw material content would have been used in ceramic production, in general. In a way, this may indicate the possibility that the potters would have made random choices in the use of raw materials.

**Table 3.** Trace elements detected in ceramics by p-XRF (ppm).

Code	Sr	Ni	Zn	Zr	Cu	Rb	Y	Nb	As	Pb	S	Br	Cr	Sb	Th	Mo
<b>SV-1</b>	496	169	154	97	76	39	27	22	18	12	-	-	485	-	-	-
<b>SV-2</b>	311	416	129	68	61	15	20	20	18	-	-	-	-	-	-	-
<b>SV-3</b>	408	241	138	63	54	14	15	11	-	-	221	2	407	-	-	-
<b>SV-4</b>	674	294	164	63	52	26	20	-	-	-	-	-	562	-	-	-
<b>SV-5</b>	272	230	139	151	71	60	30	30	14	20	-	-	407	-	-	-
<b>SV-6</b>	215	194	122	171	79	62	31	21	15	13	-	-	374	-	-	-
<b>SV-7</b>	425	423	141	56	61	17	20	-	-	-	-	-	719	-	-	-
<b>SV-8</b>	494	389	165	72	50	29	30	23	14	-	-	-	710	-	-	-
<b>SV-9</b>	472	172	105	65	52	21	11	-	-	-	-	-	638	-	-	-
<b>SV-10</b>	535	194	147	94	62	40	26	19	20	-	-	-	343	-	-	-
<b>SV-11</b>	577	191	144	84	74	33	26	15	19	12	-	-	343	83	-	-
<b>SV-12</b>	466	187	102	102	45	23	17	-	-	14	-	2	333	-	-	-
<b>SV-13</b>	416	440	114	47	74	15	18	13	-	-	-	-	719	-	-	-
<b>SV-14</b>	179	377	128	77	44	17	18	19	-	-	-	-	-	-	-	-
<b>SV-15</b>	520	405	125	50	65	16	19	13	-	-	-	-	567	-	-	-
<b>SV-16</b>	221	236	121	155	41	66	37	26	16	22	-	-	281	-	32	-
<b>SV-17</b>	325	518	196	74	96	30	29	25	23	-	-	-	769	-	-	-
<b>SV-18</b>	259	344	193	140	70	60	35	26	17	12	-	2	428	-	-	9
<b>SV-19</b>	199	239	147	186	47	67	35	30	20	18	-	-	677	-	-	-
<b>SV-20</b>	455	358	160	73	65	26	28	19	-	-	-	-	-	-	-	-
<b>SV-21</b>	342	588	166	79	85	28	27	19	24	-	-	-	926	-	-	-
<b>SV-22</b>	346	249	103	49	68	19	14	15	18	-	-	-	567	-	-	-
<b>SV-23</b>	399	272	172	114	76	46	31	18	14	-	-	-	396	-	-	-
<b>SV-24</b>	398	172	132	111	47	39	28	16	14	14	-	2	395	-	-	-
<b>SV-25</b>	554	243	147	97	79	36	30	22	16	14	-	-	409	-	-	-
<b>SV-26</b>	540	159	140	89	58	34	28	12	18	-	-	-	415	-	-	-
<b>SV-27</b>	392	612	197	74	96	23	26	15	13	12	-	1	795	-	-	-
<b>SV-28</b>	632	231	162	77	70	33	24	16	11	-	-	2	373	-	-	-
<b>SV-29</b>	241	222	130	176	65	71	34	27	14	18	-	2	312	-	-	-
<b>SV-30</b>	440	454	141	59	58	19	18	17	9	-	-	2	698	-	-	-

(-): not determined or below the detection limit.

The trace elements detected in p-XRF analysis for the ceramics are given in Table 3, and the variations of dominant ones are given in Figure 5. A classification was also made through the trace elements considering both all the trace elements (Figure 6a) and the elements (Sr, Zn, Rb, Y, Cu, Zr, Ni, Cr) excluding the ones that are not present in some samples or are below the detection limit (Figure 6b). In the classification made in terms of the oxide contents, ceramics were divided into two groups and the most decisive oxide in that grouping was CaO which indicated that calcareous raw materials were used in ceramics, but the raw material(s) varied on carbonate contents. Although it was observed that there was a relative compatibility between the classifications made through the trace elements and oxide contents, it was determined that some of the samples have replaced within the groups. This situation supported the prediction that a single source would have not been utilized in the use of raw materials.

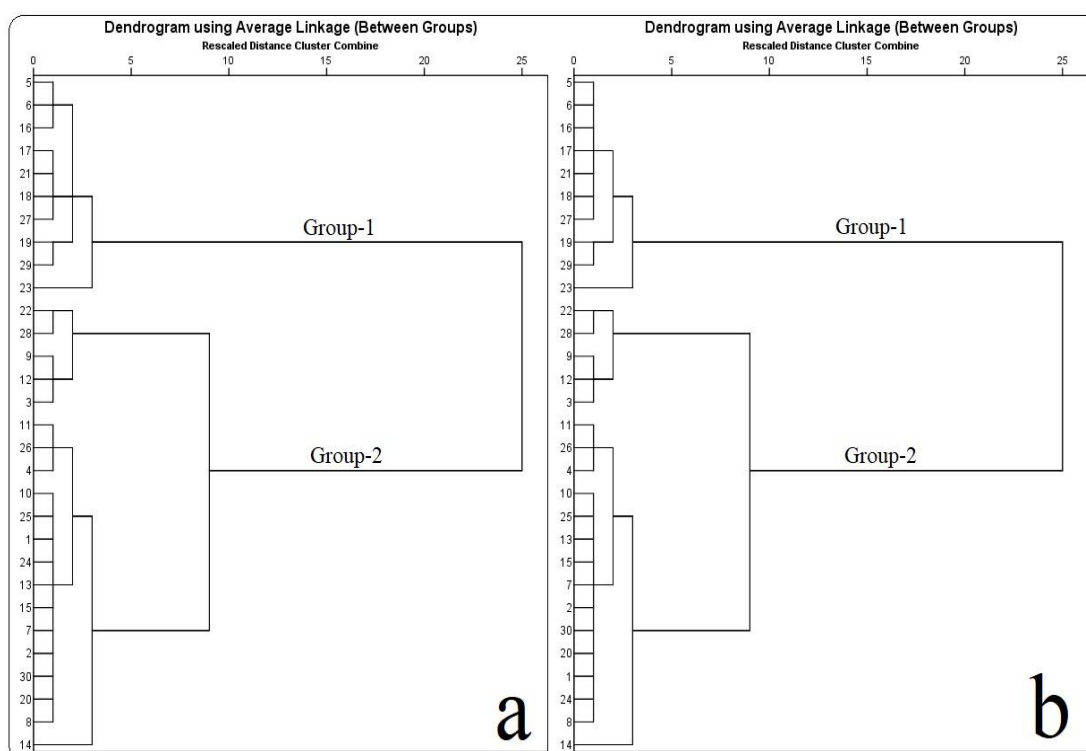


**Figure 4.** Dendrograms showing the classification made by considering (a) CaO, SiO<sub>2</sub>, Al<sub>2</sub>O<sub>3</sub>, Fe<sub>2</sub>O<sub>3</sub>, K<sub>2</sub>O and TiO<sub>2</sub>, (b) CaO, SiO<sub>2</sub> and Al<sub>2</sub>O<sub>3</sub>.

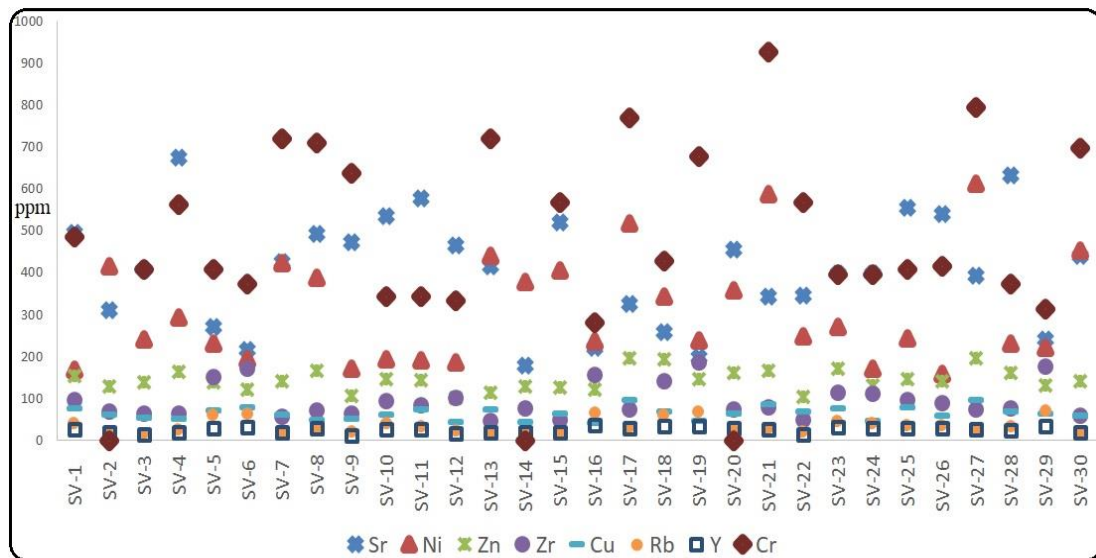


**Figure 5.** The variation of trace elements dominant in the samples.

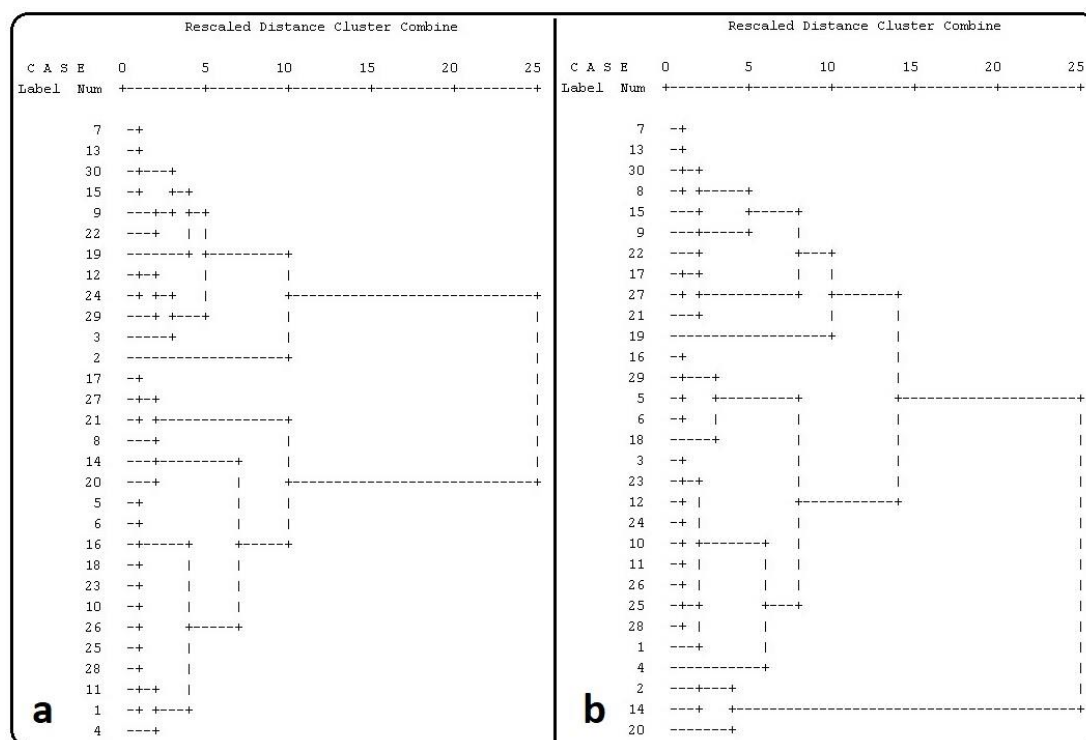


**Figure 6.** Dendrograms showing the classification made by considering (a) all trace elements identified, (b) Sr, Zn, Rb, Y, Cu, Zr, Ni, Cr.

### 3.2. XRD Results

XRD patterns of representative samples are given in Figure 7. Quartz, calcite, clay minerals, feldspar and plagioclase were detected for the whole set, while gehlenite and pyroxene were seen in few samples (Table 4). The mineralogical assemblages suggested a calcareous raw material source, and the neo-formations occasionally identified in some of the potsherds indicated a relatively higher firing temperature for such samples. Ceramics in which calcite was determined as the major mineral are SV-1, SV-2, SV-3, SV-4, SV-7, SV-9, SV-10, SV-11, SV-12, SV-13, SV-14, SV-15, SV-20, SV-22, SV-23, SV-24, SV-25, SV-26, SV-28, SV-30. Ceramic samples in which calcite was determined at lower intensities than quartz are SV-5, SV-6, SV-8, SV-16, SV-17, SV-18, SV-19, SV-21, SV-27, SV-29.

The firing temperature ranges of the ceramics were determined considering the decomposition and formation reactions of the minerals. Clay minerals tend to structurally decompose with the increasing temperature. The removal of hydroxyl groups in clay minerals can be seen around 700°C, and structural degradation around 900°C. Afterwards, the clay minerals turn into an amorphous phase and/or form new phases at higher temperatures. The structural decomposition of calcite begins ca.

700°C which might last at around 800-850°C, and the maximum temperature of calcite decomposition would vary depending on the grain size, abundance of calcite and/or the firing conditions (heating rate, firing atmosphere etc.). Dolomite decomposes at lower temperatures than calcite (i.e. ~600-700°C). Following the decomposition reactions, new phases are formed with the increasing temperature in the matrix. These are generally gehlenite (carbonated raw material + clay; ca. 800-850°C) from the melilite group and augite or diopside (carbonated raw material + quartz; ca. 850-900°C) from the pyroxene minerals [18-21].

Considering the temperature ranges of the decomposition and formation reactions of the minerals mentioned above, the evident presence of calcite in the ceramic matrix indicated that such samples were not exposed to very high temperatures (i.e. 900-1000°C). Therefore, it was predicted that the firing temperature did not exceed 800°C for the ceramics in which calcite was dominantly determined. The clay minerals detected in all samples indicated that the firing temperature of the ceramics did not exceed 900°C, while the high-temperature minerals detected in some samples pointed out that these ceramics may have been exposed to a temperature around 800-850°C, although not as high as 900°C. Even though it has been demonstrated that the high temperature minerals distinguished some of the ceramics from others (in terms of the firing temperature), the environmental conditions to which the ceramics were exposed during the firing cycle should also be taken into account. The fact that high temperature minerals generally have intensities below 50 cps on XRD patterns (except SV-2) reveals that it should not be forgotten that such minerals may be formed as a result of exposure of some ceramics to high heating rates during the firing, which would propose an uneven firing process [18-21].

**Table 4.** XRD results of the potsherds.

Sample	Mineral/phase
<b>SV-1</b>	Quartz, Calcite, Clay Mineral, Feldspar, Plagioclase
<b>SV-2</b>	Quartz, Calcite, Clay Mineral, Feldspar, Plagioclase, Gehlenite
<b>SV-3</b>	Quartz, Calcite, Clay Mineral, Feldspar, Plagioclase
<b>SV-4</b>	Quartz, Calcite, Clay Mineral, Feldspar, Plagioclase
<b>SV-5</b>	Quartz, Calcite, Clay Mineral, Feldspar, Plagioclase
<b>SV-6</b>	Quartz, Calcite, Clay Mineral, Feldspar, Plagioclase
<b>SV-7</b>	Quartz, Calcite, Clay Mineral, Feldspar, Plagioclase
<b>SV-8</b>	Quartz, Calcite, Clay Mineral, Feldspar, Plagioclase, Gehlenite
<b>SV-9</b>	Quartz, Calcite, Clay Mineral, Feldspar, Plagioclase
<b>SV-10</b>	Quartz, Calcite, Clay Mineral, Feldspar, Plagioclase
<b>SV-11</b>	Quartz, Calcite, Clay Mineral, Feldspar, Plagioclase
<b>SV-12</b>	Quartz, Calcite, Clay Mineral, Feldspar, Plagioclase
<b>SV-13</b>	Quartz, Calcite, Clay Mineral, Feldspar, Plagioclase
<b>SV-14</b>	Quartz, Calcite, Clay Mineral, Feldspar, Plagioclase, Gehlenite
<b>SV-15</b>	Quartz, Calcite, Clay Mineral, Feldspar, Plagioclase
<b>SV-16</b>	Quartz, Calcite, Clay Mineral, Feldspar, Plagioclase, Pyroxene, Gehlenite
<b>SV-17</b>	Quartz, Calcite, Clay Mineral, Feldspar, Plagioclase
<b>SV-18</b>	Quartz, Calcite, Clay Mineral, Feldspar, Plagioclase, Pyroxene, Gehlenite
<b>SV-19</b>	Quartz, Calcite, Clay Mineral, Feldspar, Plagioclase, Gehlenite
<b>SV-20</b>	Quartz, Calcite, Clay Mineral, Feldspar, Plagioclase
<b>SV-21</b>	Quartz, Calcite, Clay Mineral, Feldspar, Plagioclase
<b>SV-22</b>	Quartz, Calcite, Clay Mineral, Feldspar, Plagioclase, Gehlenite
<b>SV-23</b>	Quartz, Calcite, Clay Mineral, Feldspar, Plagioclase
<b>SV-24</b>	Quartz, Calcite, Clay Mineral, Feldspar, Plagioclase, Gehlenite
<b>SV-25</b>	Quartz, Calcite, Clay Mineral, Feldspar, Plagioclase
<b>SV-26</b>	Quartz, Calcite, Clay Mineral, Feldspar, Plagioclase
<b>SV-27</b>	Quartz, Calcite, Clay Mineral, Feldspar, Plagioclase
<b>SV-28</b>	Quartz, Calcite, Clay Mineral, Feldspar, Plagioclase
<b>SV-29</b>	Quartz, Calcite, Clay Mineral, Feldspar, Plagioclase
<b>SV-30</b>	Quartz, Calcite, Clay Mineral, Feldspar, Plagioclase

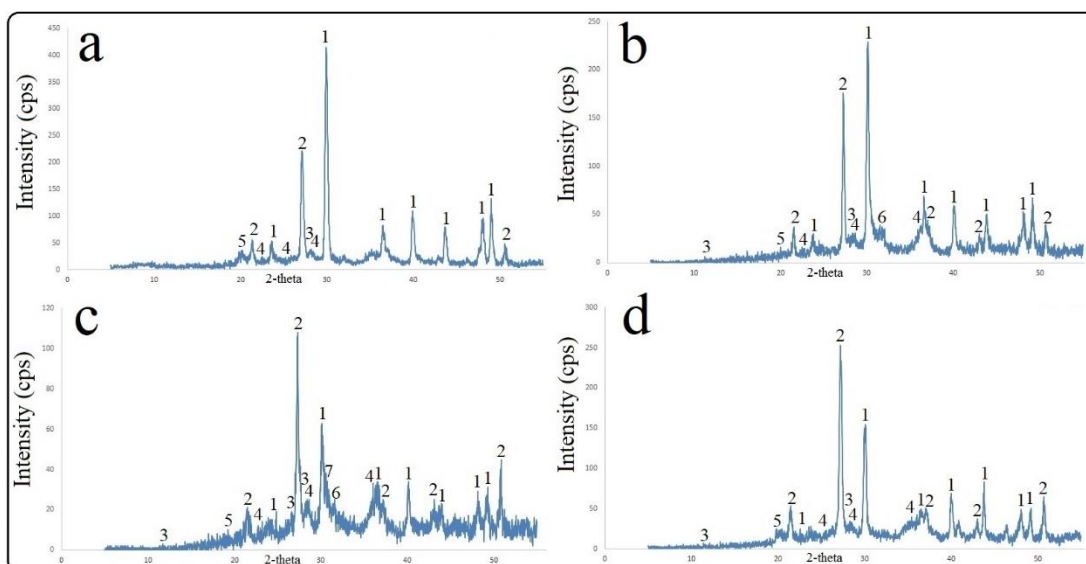


**Figure 7.** XRD patterns of representative samples (a) SV-4, (b) SV-14, (c) SV-16, (d) SV-21 (1: Calcite, 2: Quartz, 3: Feldspar, 4: Plagioclase, 5: Clay mineral, 6: Gehlenite, 7: Pyroxene).

### 3.3. Petrography results

Quartz and plagioclase were detected for the whole set, and opaque minerals, biotite and pyroxene minerals were seen in most of the samples (Table 5). In addition to the chert content detected in all samples, clay, claystone, marl (clay rich in calcium carbonate) and argillized dacite (volcanic rock with a composition between andesite and rhyolite) were occasionally determined in the sample set. The groups formed as a result of the petrographic analysis are as follows (please see Table 5);

Gr1: SV-17, SV-28

Gr2: SV-7, SV-10, SV-16, SV-27

Gr3: SV-11, SV-13, SV-15, SV-25, SV-26, SV-29

Gr4: SV-1, SV-5, SV-6, SV-18, SV-19, SV-30

Gr5: SV-2, SV-3, SV-4, SV-9, SV-12, SV-14, SV-24

Gr6: SV-8, SV-20, SV-21, SV-22, SV-23

**Table 5.** Petrography results of the ceramics.

Groups	Porosity (% in vol.)	MTA* (% in vol.)	Rock/Mineral**	Aggregate***	Rock Origin
Gr1	15	45	Q,Ch,Pl,Op,G (%2)	Very fine	Claystone
Gr2	12	29	Q,C,Ch,Pl,Op	Medium	Marl
Gr3	12	22	Q,Ch,Pl,Op,G (%1)	Fine	Clay
Gr4	12	20	Q,Ch,Pl,Bi,Py,Op,D,G (%1)	Coarse	Argillized Dacite
Gr5	15	10	Q,Ch,Pl,Bi,Py,G (%2)	Very fine	Claystone
Gr6	14	22	Q,Ch,Pl,Bi,Py,Op	Fine	Claystone

(\*) MTA: Matrix Total Aggregate,

(\*\*) Bi: Biotite, C: Calcite, Ch: Chert, D: Dacite, Op: Opaque Minerals, Pl: Plagioclase, Py: Pyroxene, Q: Quartz, G: Grog (brick particles)

(\*\*\*) Fine / Medium / Coarse Aggregate (mm): <0,5 / 0,5-1,0 / >1,0

In addition to the minerals and rock types identified in the ceramic pastes, the grog content was also revealed for some of the samples. Ceramics containing grog 1 % (in volume) are SV-1, SV-5, SV-6, SV-11, SV-13, SV-15, SV-18, SV-19, SV-25, SV-26, SV-29, SV-30. Ceramics containing grog 2 % (in volume) are SV-2, SV-3, SV-4, SV-9, SV-12, SV-14, SV-17, SV-24 SV-28. As is seen, most of the ceramics contain grog, which is thought to be preferred as a temper material in order to strengthen the ceramic body [19,22]. Grog content can be specified as ground ceramic or brick pieces, as well as the temper raw materials used in the form of clay lumps, and these types of materials could be subsequently added to the raw material and prevent the ceramic body from deforming due to water loss during the drying or firing process [19,22]. The grog content was also occasionally observed in microphotographs of the ceramics (SV-5, SV-9, SV-12, SV-14) (Figure 7). Elongated or sometimes irregularly shaped gaps, which are evident in the macro observations of the ceramics and were thought to be most likely formed as a result of the burning away of the organic materials (vegetable remains, straw, grass, etc.) during firing, were also encountered in micro-photographs (e.g. SV-2, SV-3, SV-7, SV-10, SV-19, SV-20, SV-30) (Figure 8).

In an archaeometric study for Çatalhöyük Neolithic ceramics [23], another parameter was mentioned in the use of herbal additives such as straw, which increase the binding property of clay during drying. It has been stated that the use of such easily combustible materials in the production of clay-based products can help to reach higher temperatures in a shorter time during firing. In the mentioned study, it was stated that the small (or trace) amount of gehlenite and aluminum diopside detected in the ceramic bodies were also an indicator of that prediction [23].

In the current study, the high temperature minerals determined for some of the ceramics in XRD analysis and the voids determined in the thin section analysis suggested that combustible organic additives could have increased the sensible temperature of such ceramics, and may have boosted the heating rate, as Akça et al., 2009 [23] pointed out.



**Figure 8.** Microphotographs of the ceramics.

### 3.4. FTIR results

FTIR analysis was carried out between  $650\text{-}4000\text{ cm}^{-1}$  (Figure 9), but the results were interpreted considering the range of  $650\text{-}1800\text{ cm}^{-1}$  (the fingerprint region for the ceramics). Thus, only the bands between  $650\text{-}1800\text{ cm}^{-1}$  are given in this section (all the raw results of FTIR are not given here). When the band values in the FTIR spectra were examined (Table 6), it was observed that these values were generally in harmony with the mineralogical content determined in the XRD analysis.

It was predicted that calcite, which dominantly appeared in the XRD analysis, showed peaks in the ranges of  $1412\text{-}1439\text{ cm}^{-1}$ ,  $871\text{-}877\text{ cm}^{-1}$  and  $709\text{-}716\text{ cm}^{-1}$  in the FTIR spectra. Apart from these band values, calcite was also revealed with the bands in the range of  $1440\text{-}1458\text{ cm}^{-1}$ . It was thought

that the reason for the shift of the band values from 1412 cm<sup>-1</sup> to 1458 cm<sup>-1</sup> could be secondary calcite formed in the ceramic body due to the burial conditions [19,24].

**Table 6.** Bands detected in FTIR analysis and the possible minerals assigned.

SV	Band value (cm <sup>-1</sup> )	Minerals assigned* [16, 24-34]
1	1797/1647/1430/874/798/712/691/670	C/OH/C/C,Pr,Do/Q/C/Q/Fs,P
2	1795/1636/1427/1158/873/798/779/712/667	C/OH/C/Q,Fs,P/C,Pr,Do/Q/Q/C/Fs,P
3	1795/1642/1412/872/798/778/712	C/OH/C/C,Pr,Do/Q/Q/C
4	1797/1643/1425/1003/873/798/779/712	C/OH/C/K,I,Fs,P/C,Pr,Do/Q/Q/C
5	1643/1429/875/819/796/775/716/693/672/655	OH/C/C,Pr,Do/Ch,I/Q/Q/C/Q/Fs,P/Fs,P
6	1648/1437/871/798/779/709/690/658	OH/C/C,Pr,Do/Q/Q/C/Q/Fs,P
7	1458/1166/1093/894/873/836/824/796/773/711/693/665	C/Q,G,Fs/Fs,P/I/C,Pr,Do/Ar,Do,S/Ch/Q/Q/C/Q/Fs,P
8	1797/1671/1426/1161/1016/797/773/711/688/651	C/OH/C/Q,Fs,P/K,Fs,P/Q/Q/C/Q/Fs,P
9	1797/1641/1427/1163/873/798/779/712/691	C/OH/C/Q,Fs,P/C,Pr,Do/Q/Q/C/Q
10	1652/1436/1158/1091/915/875/798/779/714/691	OH/C/Q,G,Fs/Fs,P/K,Pr/C,Pr,Do/Q/Q/C/Q
11	1428/1161/874/798/775/712/690	C/Q,G,Fs/C,Pr,Do/Q/Q/C/Q
12	1795/1435/1166/873/800/777/712/697	C/C/Q,G,Fs/C,Pr,Do/Q,K/Q/C/Q
13	1435/1163/1002/873/799/777/712	C/Q,G,Fs/K,I,Fs,P/C,Pr,Do/Q,K/Q/C
14	1441/1019/877/831/794/773/709/690/651	C/K,Fs,P/C,Pr,Do/Ar,Do,S/Q/Q/C/Q/Fs,P
15	1797/1650/1428/1163/873/799/779/712	C/OH/C/Q,G,Fs/C,Pr,Do/Q,K/Q/C
16	1643/1433/1009/874/793/775/709/690	OH/C/K,I,Fs,P/C,Pr,Do/Q,K/Q/C/Q
17	1641/1428/1165/1006/874/798/779/711/691	OH/C/Q,G,Fs/K,I,Fs,P/C,Pr,Do/Q,K/Q/C/Q
18	1424/1166/1002/873/798/777/711/693/662	C/Q,G,Fs/K,I,Fs,P/C,Pr,Do/Q,K/Q/C/Q/Fs,P
19	1654/1442/1001/875/789/772/742/695	OH/C/K,I,Fs,P/C,Pr,Do/Q,K/Q/Fs,P/Q
20	1795/1643/1434/1019/877/797/775/712/691	C/OH/C/K,Fs,P/C,Pr,Do/Q,K/Q/C/Q
21	1640/1440/1163/1004/874/798/777/712	OH/C/Q,G,Fs/K,I,Fs,P/C,Pr,Do/Q,K/Q/C
22	1795/1645/1428/1002/875/798/775/712/693	C/OH/C/K,Fs,P/C,Pr,Do/Q,K/Q/C/Q
23	1643/1438/1163/874/796/779/711/691	OH/C/Q,G,Fs/C,Pr,Do/Q,K/Q/C/Q
24	1799/1645/1428/1009/874/796/777/711/693	C/OH/C/K,Fs,P/C,Pr,Do/Q,K/Q/C/Q
25	1443/1016/875/798/777/711/691	C/K,Fs,P/C,Pr,Do/Q,K/Q/C/Q
26	1797/1641/1428/1006/873/798/779/712/691	C/OH/C/K,Fs,P/C,Pr,Do/Q,K/Q/C/Q
27	1643/1458/1439/1156/1102/1013/875/798/775/711/693/655	OH/C/C/Q,G,Fs/P,Pr/K,I,Fs,P/C,Pr,Do/Q,K/Q/C/Q/Fs,P
28	1793/1441/1166/1013/874/798/775/712/693/674	C/C/Q,G,Fs/K,I,Fs,P/C,Pr,Do/Q,K/Q/C/Q/Pr
29	1452/1008/873/798/773/737/712/691	C/K,Fs,P/C,Pr,Do/Q,K/Q/Fs,P,M/C/Q
30	1797/1645/1428/1159/1076/1002/873/798/777/712/693/667	C/OH/C/Q,G,Fs/Q,Pr,M/K,Fs,P/C,Pr,Do/Q,K/Q/C/Q/Fs,P

\* A: Aragonite, C: Calcite, Ch: Chlorite, Do: Dolomite, Fs: Feldspar, G: Gypsum, I: Illite,

K: Kaolinite, M: Muscovite, OH: H-O-H stretches, P: Plagioclase, Pr: Pyroxene, S: Sanidine

The band values in the range of 1000-1019  $\text{cm}^{-1}$  were attributed to the clay minerals, while the bands in the range of 1158-1166  $\text{cm}^{-1}$ , 794-800  $\text{cm}^{-1}$ , 772-779  $\text{cm}^{-1}$  and 688-697  $\text{cm}^{-1}$  indicated the existence of quartz. It should not be ignored that the bands in the range of 1158-1166  $\text{cm}^{-1}$  pointing to quartz may be also indicative of feldspar/plagioclase minerals. This type of band overlapping is likely to be encountered in FTIR spectra. The band values of 1636-1647  $\text{cm}^{-1}$ , 1650-1654  $\text{cm}^{-1}$  and 1671  $\text{cm}^{-1}$  were assigned to OH<sup>-</sup> vibrations (H-O-H stretches) which suggested the presence of hygroscopic water in ceramic paste [16, 24-34].

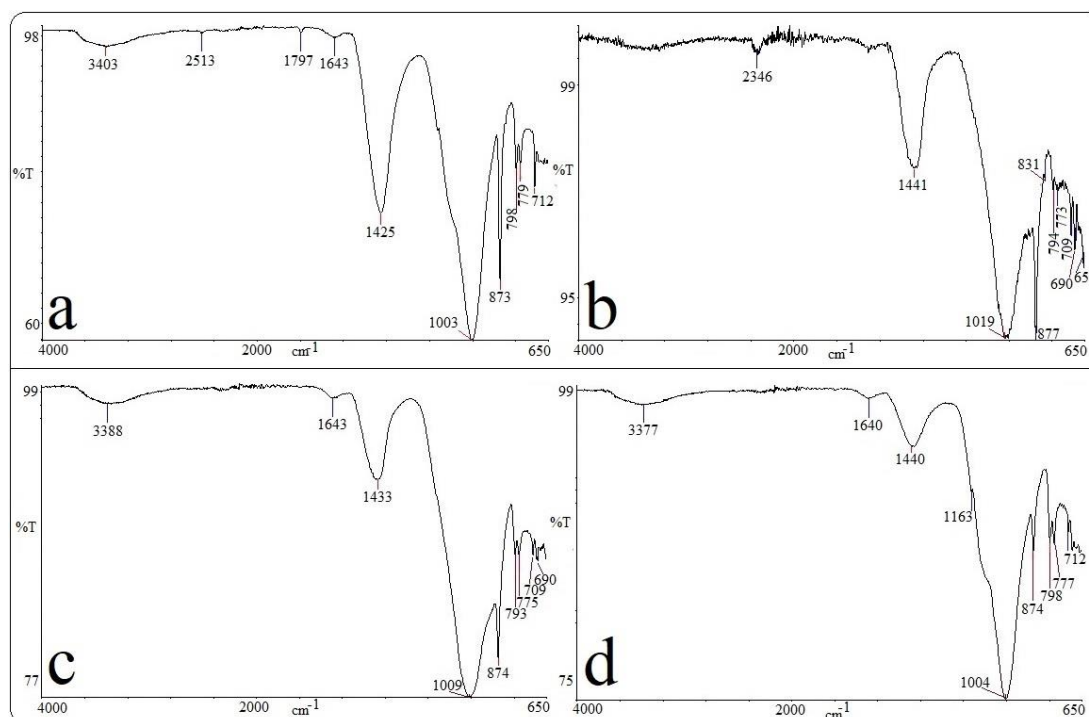


**Figure 9.** FTIR spectra of representative samples (a) SV-4, (b) SV-14, (c) SV-16, (d) SV-21.

#### 4. CONCLUSIONS

The pottery recovered from the Şah Valley hillside settlement represents the easternmost examples of Hassuna Samarra, and this research has focused on Neolithic ceramic findings belonging to that culture. The chemical composition and mineralogical assemblage of the samples indicated to use of calcareous raw materials. The geological structure rich in carbonated raw materials in and around the province of Şırnak indicates that the high CaO content is likely of regional origin [35-39]. In XRF analysis, it was determined that iron was the main element in formation of the reddish colors in

ceramic bodies. The elongated and irregular voids, which were clearly observed on most of the ceramic surfaces and were predicted to be formed as a result of the removal of organic materials by burning, suggested that organic materials would be as effective as iron in formation of sandwich structure. The voids on the potsherds can also be caused by wheel construction or partial loss of calcite. Considering the fact that the potsherds belong to the Neolithic Period, use of wheel could be ignored and partial loss of calcite may be evaluated as a valid parameter in occurrence of the gaps, in addition to the probable presence of organic additives [40].

In the hierarchical clustering analysis performed through the statistical program SPSS (considering the chemical composition of the ceramics), it was revealed that the starting raw materials used in the production of ceramics generally contain calcium, magnesium, silica and alumina. In the statistical analyses, ceramics were divided into two groups and CaO was decisive in the formation of these groups. The results indicated that sources varying in carbonated raw material contents would have been used in ceramic production, in general. In the clustering analysis carried out with the trace elements, the displacement of some samples between the former groups (created depending on the main oxides) indicated that more than one source would have been used in preparation of the starting materials.

Taking into account the temperatures of decomposition and formation reactions of the minerals, it was revealed that the ceramics were mostly fired at temperatures not exceeding 800°C. In FTIR analysis, which was applied as a complementary technique in the study, the data were compatible with the XRD patterns. In petrography analysis, which was another method of determining the mineral content, quartz and plagioclase were detected for the whole set, and opaque minerals (hematite, magnetite, etc.), biotite and pyroxene minerals were detected in most of the samples. Grog, which was thought to be preferred as a temper material in most of the ceramics, has been detected and it was predicted that this content might have been subsequently added to the paste to prevent the ceramic from deforming due to water loss during the drying and firing processes.

Six groups were revealed in petrographic investigation which re-assorted the potsherds unlike the first grouping made in XRF analysis. It was also seen that the potsherds possessing calcite at lower intensities than quartz in XRD were mostly in compatible with Group-1 emerged in XRF analysis (except SV-23), while the potsherds having calcite as the dominant mineral in XRD were mostly compatible with Group-2 revealed in XRF analysis (except SV-8). These results suggested that the chemical and mineralogical contents were coherent and there would have been more than one raw material source which may indicate use of different clay batches by the potters. Such prediction would also point out there could be different pottery ateliers, instead of a single production center.

Within this research, a detailed archaeometric database is created for the Neolithic ceramics of Şah Valley. It is thought that the results of this work would be directive for the further studies on Neolithic ceramics in Anatolia. In addition to this research, provenance studies can be carried out using clay samples supplied from the region.

## **ACKNOWLEDGEMENTS**

We gratefully thank Assoc. Prof. Dr. Ali Akın Akyol (Ankara Hacı Bayram Veli University), Prof. Dr. Yusuf Kağan Kadioğlu and Assist. Prof. Dr. Kıymet Deniz (Ankara University, Earth Sciences Application and Research Center; YEBİM), Assoc. Prof. Dr. Sema Tetiker and Assoc. Prof. Dr. Mahmut Aydın (Batman University), and Gülşen Albuz Geren (Ankara Hacı Bayram Veli University, Materials Research and Conservation Laboratory; MAKLAB) for their support in application of the analytical techniques. We also thank the laboratories for preparation of the samples and application of the analyses; Dicle University Science and Technology Application and Research Center, Batman University Central Research Laboratory, Ankara University Earth Sciences Application and Research Center, Ankara Hacı Bayram Veli University Materials Research and Conservation Laboratory. This paper covers the data of the master thesis submitted by Esra Kaynak to the Department of Archaeometry at the Institute of Science, Batman University (2019).

## **REFERENCES**

- [1] Eramo, G., Laviano, R., Muntoni, I. M. and Volpe, G. (2004). Late Roman cooking pottery from the Tavoliere area (Southern Italy): raw materials and technological aspects. *Journal of Cultural Heritage*, 5(2), 157-165.
- [2] Arcasoy, A. (1983). *Seramik Teknolojisi*, Marmara Üniversitesi Yayınları, İstanbul.
- [3] Bayazit, M., Adsan, M., Genç, E. (2020). Application of spectroscopic, microscopic and thermal techniques in archaeometric investigation of painted pottery from Kuriki (Turkey). *Ceramics International*, 46, 3695-3707.
- [4] Bayazit, M. and Akyol, A.A. (2015). Medeniyetler arasındaki etkileşim köprüsü: seramik (arkeometrik yaklaşım), 9. Uluslararası Eskişehir Pişmiş Toprak Sempozyumu, 5-20 Eylül 2015, Eskişehir, 69-78.
- [5] Bayram, G. (2018). Güneydoğu Anadolu'nun Neolitik Çağ totemleri ve ritüel nesnelere. *AMISOS*, 3(4), 67-89.
- [6] Özüşen, B. and Yıldız, Z. (2012). Buzul Çağı'ndan İlk Çağ'a Tüketimin Tarihi. *Süleyman Demirel Üniversitesi Vizyoner Dergisi*, 4(7), 1-16.
- [7] Efecan, S. (2011). Geç Neolitik Döneme ait Hacılar Kazılarında Bulunmuş Terracota Figürlerin Çağdaş Yorumlarla Biçimlendirilmesi, Yüksek Lisans Tezi, Arkeoseramik Anasanat Dalı, Güzel Sanatlar Enstitüsü, Süleyman Demirel Üniversitesi.
- [8] Coşkun, N., Ayman, İ., Yumruk, Ş. and Aşkar, İ.T. (2019). 2017 Yılı Şırnak İli Merkez, Güçlükonak, Uludere ve Beytüşşebap İlçeleri Yüzey Araştırması, 36. Araştırma Sonuçları Toplantısı (7-11 Mayıs 2018, Çanakkale), Ankara, 175-194.

- [9] Erinç S. (1980). Kültürel çevre bilim açısından Güneydoğu Anadolu. In H. Çambel and R.J. Braidwood (Eds.), *Güneydoğu Anadolu Tarihöncesi Araştırmaları*, İÜ Edebiyat Fakültesi, İstanbul, pp. 65-72.
- [10] Çelik, B. (2010). Şırmak ve çevresinin obsidyen ticaretinde yeri ve önemi. *Anadolu / Anatolia* 36, 1-11.
- [11] Yakar, J. (2007). *Anadolu'nun Etnoarkeolojisi: Tunç ve demir çağlarında kırsal kesimin sosyo-ekonomik yapısı* (çev. S.H. Riegel, ed. B. Avunç), Homer Kitabevi.
- [12] Tekin, H. (2015). Yukarı Mezopotamya'nın ilk boyalı çanak-çömlekleri: Hassuna, Samarra ve Halaf: yeni yorumlar ve yaklaşımlar. Bölüm 1: Hassuna ve Samarra. *OLBA*, 23, 1-57.
- [13] Tekin, H. (2017). *Tarihöncesinde Mezopotamya: Yeni yaklaşımlar, yeni yorumlar ve yeni kronoloji*, Bilgin Kültür Sanat Yayınları, Ankara, 476 p.
- [14] Bayazit, M. (2018). Archaeometric study of possible Ninevite-5 pottery from upper Tigris region using SEM-EDS, PEDXRF, and OM. *X-Ray Spectrometry*, 47, 92-104.
- [15] Kibaroğlu, M. (2005). Sedimentary geochemical approach to the provenance of the noncalciferous north Mesopotamian Metallic Ware. *Archeometriai Muhely*, 2, 48-51.
- [16] İssi, A. (2012). Estimation of ancient firing technique by the characterization of semi-fused Hellenistic potsherds from Harabebezikan/Turkey. *Ceramics International*, 38 (3), 2375-2380.
- [17] Bong, W.S.K., Matsumura, K. and Nakai, I. (2008). Firing technologies and raw materials of typical early and middle Bronze Age pottery from Kaman-Kalehöyük: a statistical and chemical analysis. *Anatol. Archaeol. Stud.*, 17, 295-311.
- [18] Cultrone, G., Rodriguez-Navarro, C., Sebastian, E., Cazalla, O. and De La Torre, M.J. (2001). Carbonate and silicate phase reactions during ceramic firing. *Eur. J. Miner.* (13), 621-634.
- [19] Fabbri, B., Gualtieri, S. and Shoval, S. (2014). The presence of calcite in archeological ceramics. *J. Eur. Ceram. Soc.*, 34, 1899-1911.
- [20] Broekmans, T., Adriaens, A. and Pantos, E. (2004). Analytical investigations of cooking pottery from Tell Beydar (ne-Syria). *Nuclear Instruments & Methods in Physics Research Section B*, 226, 92-97.
- [21] Shoval, S., Gaft, M., Beck, P. and Kirsh, Y. (1993). The thermal behavior of limestone and monocrySTALLINE calcite tempers during firing and their use in ancient vessels. *J. Therm. Anal.*, 40, 263-73.

- [22] Rice P.M. (1987). Pottery analysis: A sourcebook, University of Chicago Press, Chicago, 584p.
- [23] Akça, E., Kapur, S., Özdöl, S., Hodder, I., Poblome, J., Arocena, J., Kelling, G. and Bedestenci, Ç. (2009). Clues of production for the Neolithic Çatalhöyük (central Anatolia) pottery. *Scientific Research and Essays*, 4(6), 612-625.
- [24] Mazzocchin, G.A., Agnoli, F. and Colpo, I. (2003). Investigation of roman age pigments found on pottery fragments. *Analytica Chimica Acta* (478), 147-161.
- [25] Gadsden, J.A. (1975). *Infrared Spectra of Minerals and Related Inorganic Compounds*, Butterworth & Co Publishers, London, 277 p.
- [26] Iglesias, J.E. and Serna, C.J. (1985). The IR spectra of hematite-type compounds with different particle shapes. *Miner. Petrogr. Acta*, 29A, 363-370.
- [27] Palanivel, R. and Velraj, G. (2007). FTIR and FT-Raman spectroscopic studies of fired clay artifacts recently excavated in Tamilnadu, India. *Indian Journal of Pure and Applied Physics*, 45, 501-508.
- [28] Faust, G.T. (1953). Huntite,  $Mg_3Ca(CO_3)_4$ , a New Mineral. *American Mineralogist*, 38, 4-24.
- [29] Farmer, V.C. (1974). *Infrared Spectra of Minerals*, Ed. Mineralogical Society, London, 539 p.
- [30] Ion, R.M., Dumitriu, I., Fierascu, R.C., Ion, M.L., Pop, S.F., Radovici, C., Bunghez, R.I. and Niculescu, V.I.R. (2011). Thermal and mineralogical investigations of historical ceramic, A case study. *J Therm Anal Calorim*, 104, 487-493.
- [31] De Benedetto, G.E, Laviano, R., Sabbatini, L. and Zambonin, P.G. (2002). Infrared spectroscopy in the mineralogical characterization of ancient pottery. *Journal of Cultural Heritage*, 3, 177-186.
- [32] Ellid, M.S., Murayed, Y.S., Zoto, M.S., Music, S. and Popovi, S. (2003). Chemical reduction of hematite with starch. *Journal of Radioanalytical and Nuclear Chemistry*, 258 (2), 299-305.
- [33] <http://rruff.info/> (Access date 30.05.2019).
- [34] Maravelaki-Kalaitzaki, P. and Kallithrakas-Kontos, N. (2003). Pigment and terracotta analyses of Hellenistic figurines in Crete. *Analytica Chimica Acta* 497, 209-225
- [35] Maden Tetkik ve Arama Genel Müdürlüğü. “İl Maden Haritaları-Şırnak”, 29.04.2019, <http://www.mta.gov.tr/v3.0/sayfalar/hizmetler/maden-haritalari/Sirnak.pdf>
- [36] Maden Tetkik ve Arama Genel Müdürlüğü. “İl Maden Haritaları-Mardin”, 29.04.2019, <http://www.mta.gov.tr/v3.0/sayfalar/hizmetler/maden-haritalari/mardin.pdf>

- [37] Maden Tetkik ve Arama Genel Müdürlüğü. “İl Maden Haritaları-Batman”, 29.04.2019, <http://www.mta.gov.tr/v3.0/sayfalar/hizmetler/maden-haritalari/batman.pdf>
- [38] Maden Tetkik ve Arama Genel Müdürlüğü. “İl Maden Haritaları-Van”, 29.04.2019, <http://www.mta.gov.tr/v3.0/sayfalar/hizmetler/maden-haritalari/Van.pdf>
- [39] Maden Tetkik ve Arama Genel Müdürlüğü. “İl Maden Haritaları-Hakkari”, 29.04.2019, <http://www.mta.gov.tr/v3.0/sayfalar/hizmetler/maden-haritalari/hakkari.pdf>
- [40] Semiz, B., Duman, B. (2017). Tripolis’te bulunan Geç antik Çağ Unguentariumları’nın Arkeometrik yönden değerlendirilmesi, Tripolis ad Maeandrum I, Tripolis arařtırmaları (Ed.: Duman, B.), Ege Yayınları, 165-180.